Article

Effect of Fumonisin B1 on Proliferation and Apoptosis of Intestinal Porcine Epithelial Cells

Tianjie Wang [†], **Hongyu Lei** [†], **Lihua Zhou, Meiwen Tang, Qing Liu, Feng Long, Qing Li and Jianming Su** *

Provincial Key Laboratory of Protein Engineering in Animal Vaccines College of Veterinary Medicin, Hunan Agricultural University, Changsha 410128, China; tjwang@stu.hunau.edu.cn (T.W.); leihy77@hunau.edu.cn (H.L.); zlh240141@163.com (L.Z.); 1737151498@stu.hunau.edu.cn (M.T.); liuqingqing@stu.hunau.edu.cn (Q.L.); 1499685240@stu.hunau.edu.cn (F.L.); qingli@stu.hunau.edu.cn (Q.L.)
* Correspondence: sjmauhn@hunau.edu.cn
† These authors contributed equally to this work.

Abstract: Fumonisin B_1 (FB_1), which is a mycotoxin produced by *Fusarium moniliforme* and *Fusarium rotarum*, has a number of toxic effects in animals. Moldy feed containing FB_1 can damage the intestine. In this study, we used intestinal porcine epithelial cells (IPEC-J2) as an in vitro model to explore the effects of FB_1 on cell cycle and apoptosis. The results showed that IPEC-J2 cells treated with 10, 20, and 40 μg/mL FB_1 for 48 h experienced different degrees of damage manifested as decreases in cell number and viability, as well as cell shrinkage and floating. In addition, FB_1 reduced cell proliferation and the mRNA and protein expression of proliferating cell nuclear antigen (PCNA), cyclin-dependent kinase 2 (CDK2), CDK4, cyclinD1, and cyclinE1. FB_1 blocked the cell cycle in the G1 phase. FB_1 also induced mitochondrial pathway apoptosis, reduced mitochondrial membrane potential, and promoted mRNA and protein expression of Caspase3, Caspase9, and Bax. The findings suggest that FB_1 can induce IPEC-J2 cell damage, block the cell cycle, and promote cell apoptosis.

Keywords: Fumonisin B_1; intestinal porcine epithelial cells; apoptosis; cell proliferation

Key Contribution: This study demonstrated that FB_1 could inhibit proliferation and promote apoptosis of IPEC-J2, which helps us understand the toxic mechanisms of FB_1.

1. Introduction

Mycotoxins produced by fungi are considered as contaminants in animal feed [1]. Fumonisin B_1 (FB_1) is produced by Fusarium verticillioides, Fusarium proliferatum, and other Fusarium species; it is often found in corn [2]. FB_1 has been classified as a group 2B hazard by international research institutions [3] due to its global distribution and its harmful effects in humans and animals [4]. The gastrointestinal system is the first barrier against ingested toxins [5]. Following ingestion of FB_1-contaminated food or feed, the intestinal epithelium will be continuously exposed to high levels of FB1 [6]. Intestinal exposure to FB1 can lead to villous fusion and atrophy in the intestines of pigs [5]. In addition, FB1 impairs the establishment of the epithelial barrier and disrupts epithelium that is already established [7]. These injuries not only cause intestinal dysfunction but also promote FB_1 entering the circulatory system. As FB_1 spreads via the circulatory system throughout the body, it can damage other organs, leading to a variety of diseases.

Cell proliferation is one of the basic life activities involved in homeostasis, and the process proceeds through a sequence of stages known as the cell cycle [8]. The cell cycle is divided into a synthesis phase (S), two intervening gap phases (G1 and G2), and a mitotic segregation phase (M) [9]. Whether the cell cycle progresses smoothly has important effects on cell proliferation and apoptosis. A variety of proteins are involved in cell proliferation and regulation of the cell cycle [10], including proliferating cell nuclear antigen (PCNA), cyclin-dependent kinases (CDKs), and CDK inhibitor (CKI) [11,12]. Cyclin D can interact

with CDK4 and CDK6 to form a cyclin D-CDK4/6 complex. The cyclin D-CDK4/6 complex regulates the cell cycle by targeting pocket proteins (RB, P107, P130) [13]. Many foreign substances such as bacteria, viruses, and toxins may affect cell proliferation and cycle progression. As a result, FB1 is likely to affect the activation and interaction of cycle-related proteins, further arresting the cell cycle [14].

Apoptosis, which is a form of programmed cell death, functions to maintain systemic balance. Morphological hallmarks of apoptosis include cell shrinkage, membrane blebbing, nuclear condensation, and DNA fragmentation [15]. Classical biochemical markers of apoptosis include activation of proteases, caspases, and mitochondrial outer membrane permeabilization (MOMP). The Bcl-2 family, Apaf-1, and the caspase family in mammals are major components of the mitochondrial apoptosis pathway [16]. In the mitochondrial pathway, the critical event is a change in permeability of the outer mitochondrial membrane (OMM) resulting in the release of cytochrome C into the cytoplasm. When proteins released from mitochondria enter the cytoplasm, they activate apoptosis-related genes such as Caspase9 and Caspase3 and thus induce apoptosis [17].

Recent studies by us have shown that FB1 interferes with the expression of nutrient transporter genes in intestinal porcine epithelial cells (IPEC-J2) [18]. Moreover, FB_1 inhibits the expression of tight-junction proteins by destroying the barriers [19]. In this study, we will explore the effects of FB_1 on cell proliferation and apoptosis, and whether FB_1 affects cell apoptosis through the mitochondrial pathway.

2. Results

2.1. FB_1 Reduced the Viability of IPEC-J2 Cells and Caused Cell Damage

Cell survival was measured 24 and 48 h after IPEC-J2 cells were exposed to FB_1 (Figure 1a). Cells exposed to FB_1 at 10, 20, and 40 µg/mL for 24 h showed no significant changes in cell viability. After exposure to FB_1 at 20 and 40 µg/mL for 48 h, cell viability decreased to 95.14% and 83.66%, respectively. Cell morphology was observed under a microscope after 24 h exposure to FB_1 (Figure 1b,c). As the concentration of FB_1 increased, the number of cells gradually decreased; the cells shrank, becoming rounded and floating. This suggests that FB_1 could reduce cell survival and cause cell damage.
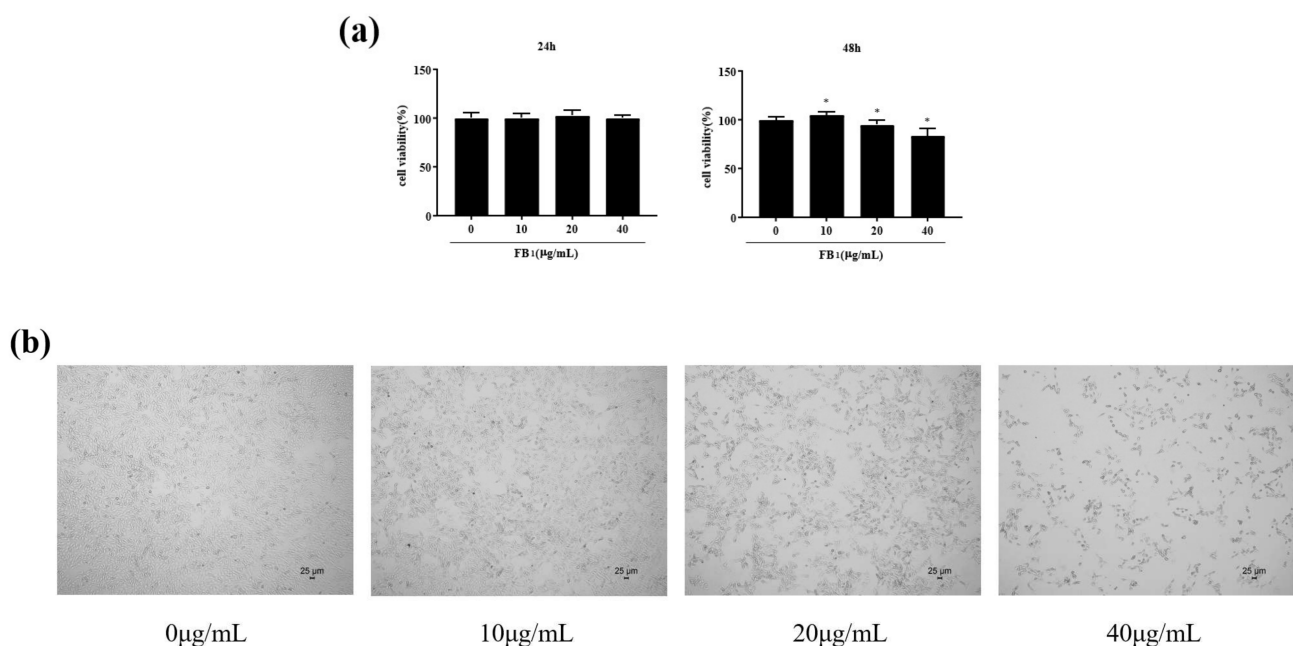
(a)

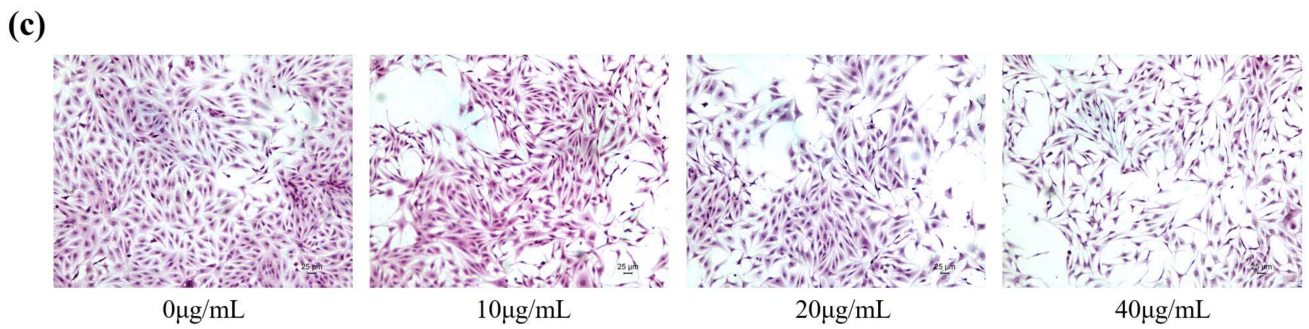**(b)**

0µg/mL   10µg/mL   20µg/mL   40µg/mL

Figure 1. *Cont*.

(c)

0μg/mL 10μg/mL 20μg/mL 40μg/mL

Figure 1. FB$_1$ reduced cell viability. (**a**) The changes in cell viability after 24 and 48 h exposure to FB$_1$ were detected (40×). (**b**) The morphological changes of cells treated with FB$_1$ (0, 10, 20, and 40 μg/mL) for 48 h were observed under a microscope. (**c**) Cell morphology was observed by HE staining (100×). The data are expressed as mean ± SD. * $p < 0.05$.

2.2. FB$_1$ Decreased Cell Proliferation and Arrested the Cell Cycle

After 48 h of treatment with different concentrations of FB$_1$, the fluorescence intensity of the 20 and 40 μg/mL FB$_1$ treatment groups decreased continuously (Figure 2a), especially in the 40 μg/mL FB$_1$ group. This indicated that the proliferation of IPEC-J2 cells was significantly inhibited with the increase in FB$_1$ concentration after treatment for 48 h.
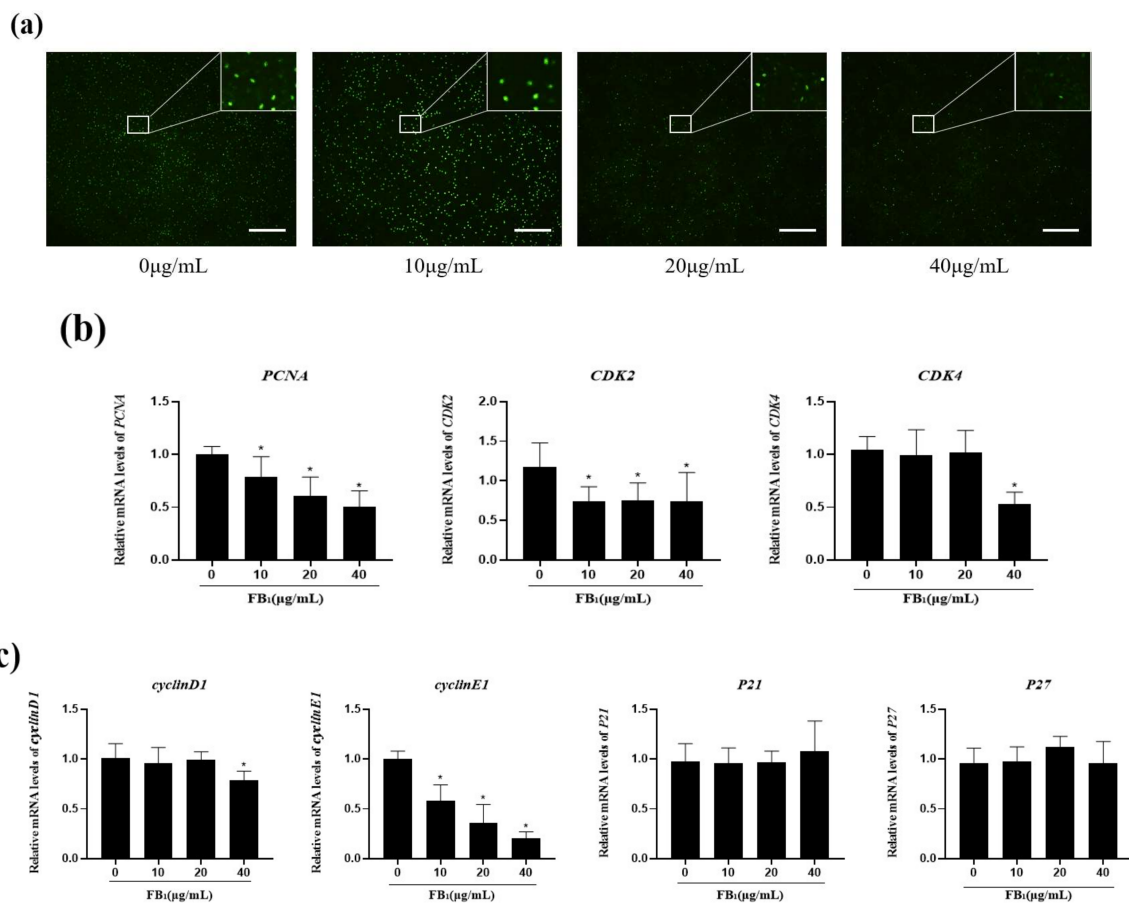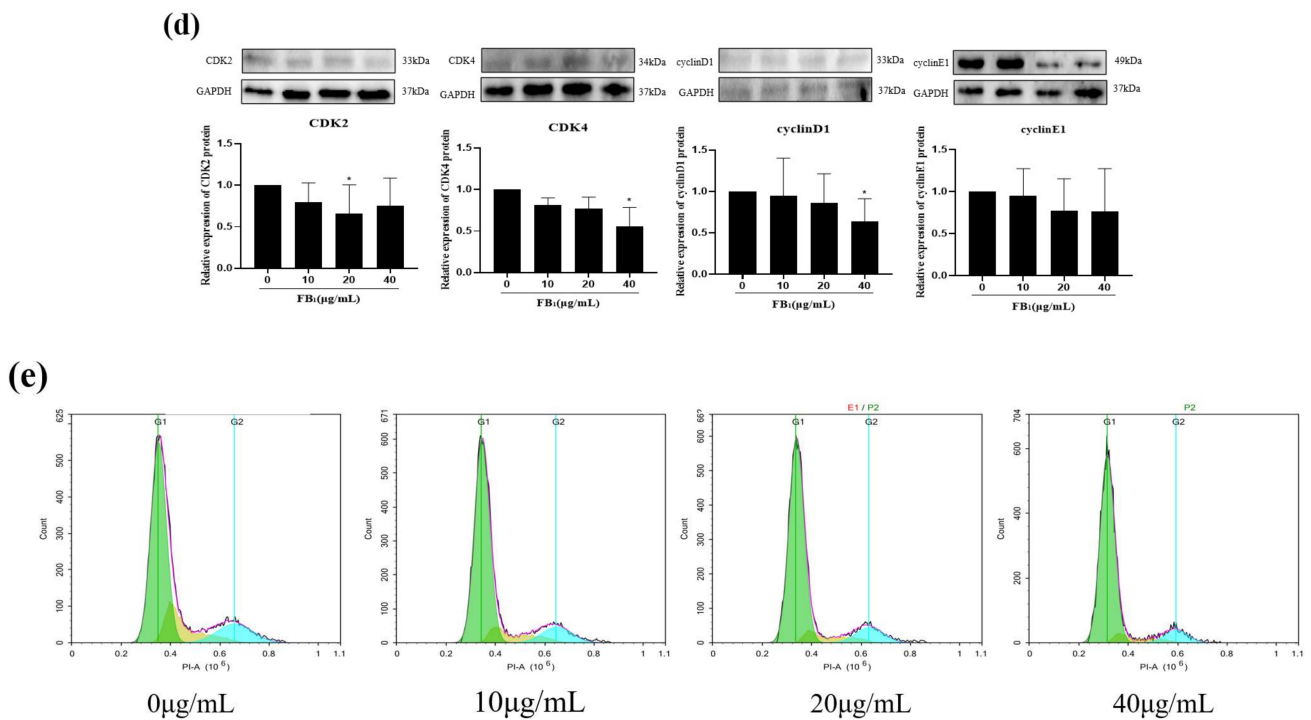
(a)

0μg/mL 10μg/mL 20μg/mL 40μg/mL

(b)

(c)

Figure 2. *Cont.*

(d)

(e)

0µg/mL   10µg/mL   20µg/mL   40µg/mL

Figure 2. FB$_1$ inhibits cell proliferation by blocking the cell cycle. (**a**) EdU analysis of the effect of FB$_1$ on cell proliferation (40×). Scale bars: 50 µm. (**b**) The effects of FB$_1$ on *PCNA*, *CDK2*, and *CDK4* mRNA were detected by qPCR. (**c**) The effects of FB$_1$ on *cyclinD1*, *cyclinE1*, *P21*, and *P27* mRNA were detected by qPCR. (**d**) The effects of FB$_1$ on cleaved CDK2, CDK4, cyclinD1 and cyclinE1 protein expression were measured. (**e**) Flow detection diagram of the cell cycle of IPEC-J2 treated with FB$_1$ for 48 h. The data are expressed as mean ± SD. * $p < 0.05$.

To further verify the effect of FB1 on cell proliferation, mRNA expression levels of PCNA, cyclin-dependent kinase inhibitors P21 and P27, cyclin-dependent kinases 2 and 4, cyclin D1 and cyclin E1 were detected (Figure 2b,c). The mRNA expression levels of PCNA and CyclinE1 decreased in a concentration-dependent manner. CDK2 expression decreased significantly under different concentrations of FB$_1$. CDK4, and CyclinD1 mRNA expression levels decreased significantly after the 40 µg/mL FB$_1$ treatment. The mRNA expression levels of P21 and P27 slightly increased in the 40 µg/mL FB$_1$ group and the 20 µg/mL FB$_1$ group. Meanwhile, the protein expression of CDK2 was significantly decreased in 20 µg/mL group, the expression of CDK4 acyclinD1 was significantly decreased in 40 µg/mL group (Figure 2d). Flow cytometry results showed that after FB$_1$ treatment, the percentage of G1 phase cells increased from 65.51% to 83.55%, while the percentage of S phase cells decreased from 18.88% to 7.08%, and there was no significant change in the number of G2 phase cells. (Figure 2e) These results indicated that FB$_1$ could inhibit the expression of G1/S phase-related genes, promote the mRNA expression of the cycle suppressor genes P21 and P27, block the cell cycle in G1 phase, and thus inhibit cell proliferation.

2.3. FB$_1$ Reduced Mitochondrial Membrane Potential and Promoted Cell Apoptosis

Mitochondria are the main production sites of cell metabolism, and their function is important for maintaining normal cell development. JC-1 was used to reflect the changes in mitochondrial membrane potential (Figure 3a). The results showed that the red fluorescence intensity increased in the 10 µg/mL FB$_1$ group but decreased in the 20 µg/mL and 40 µg/mL FB$_1$ groups. Compared with the control group, the intensity of green fluorescence increased gradually, being extremely significant in the 20 µg/mL FB$_1$ group and the

40 µg/mL FB$_1$ group, suggesting that FB$_1$ treatment could cause mitochondrial damage and loss of mitochondrial membrane potential in IPEC-J2 cells.
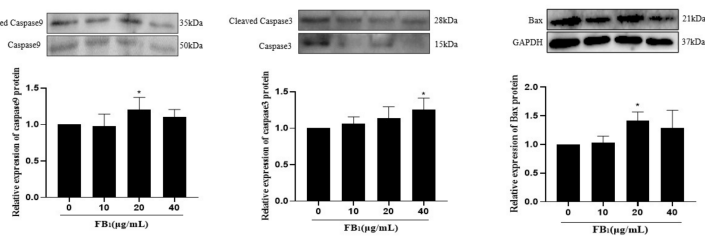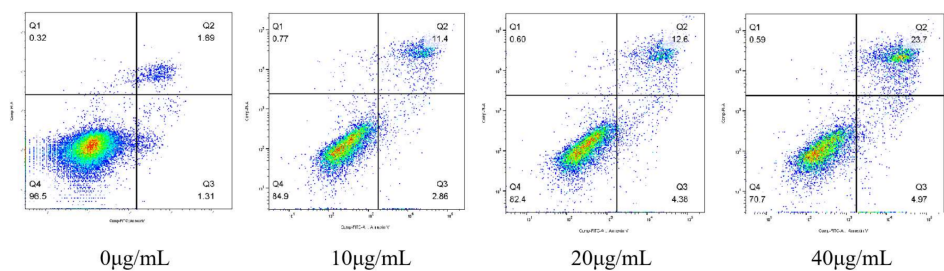
(a)

(b)

(c)

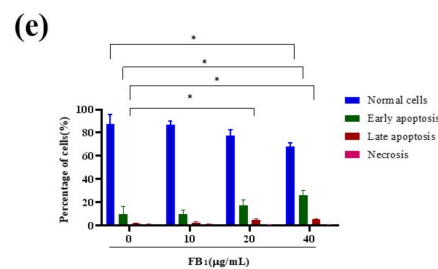
(d)

Figure 3. *Cont.*

(e)
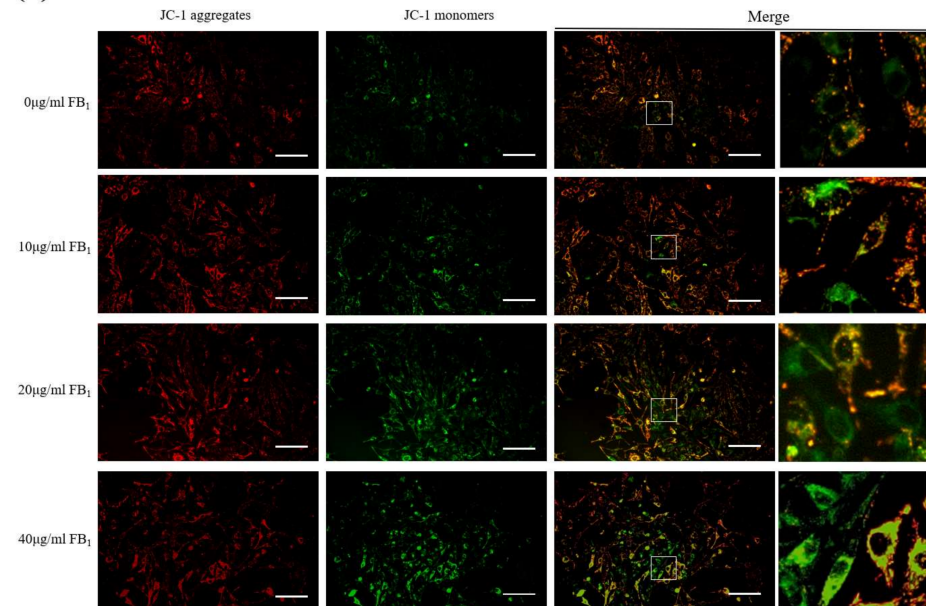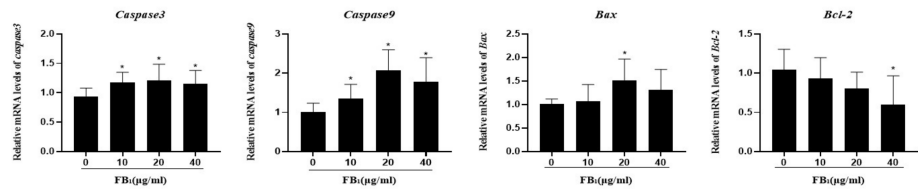
Figure 3. FB_1 reduced $\Delta\psi$m and promoted cell apoptosis. (**a**) The effects of different concentrations of FB_1 on mitochondrial membrane potential were detected by JC-1 (200×). Scale bars: 50 μm. (**b**) The effects of FB_1 on *Caspase3*, *Caspase9*, *Bax*, and *Bcl-2* mRNA were detected by qPCR. (**c**) The effects of FB_1 on cleaved Caspase9, cleaved Caspase3, and Bax protein expression were measured. (**d**) The apoptosis of IPEC-J2 cells after FB_1 treatment was analyzed by flow cytometry. (**e**) The proportion changes of IPEC-J2 normal cells, early apoptotic cells, late apoptotic cells, and necrotic cells after FB_1 treatment were measured by flow cytometry. The data are expressed as mean $\pm$ SD. * $p < 0.05$.

qPCR and Western blots were used to examine mRNA transcription levels and protein expression levels of pro-apoptotic genes *Caspase3*, *Caspase9*, *Bax* and the anti-apoptotic gene *Bcl-2* (Figure 3b). With the increase in FB_1 concentration, mRNA and protein expression levels of *Caspase3*, *Caspas9*, and *Bax* gradually increased, and the mRNA transcription levels reached a peak at 20 μg/mL. The mRNA expression of *Bcl-2* decreased with the increase in FB_1 concentration. Meanwhile, in terms of protein expression, the expression levels of cleaved Caspase9 and Bax increased significantly in the 20 μg/mL group, while the concentration of cleaved Caspase3 reached a peak at 40 μg/mL (Figure 3c). Flow cytometry showed that the proportions of early and late apoptotic cells increased in a concentration-dependent manner (Figure 3d,e). In particular, the proportion of apoptotic cells increased from 1.89% to 23.7%, while the proportion of living cells decreased from 96.5% to 70.7%. These results suggested that FB_1 could promote the apoptosis of IPEC-J2 cells through the endogenous apoptosis pathway.

3. Discussion

As a common mycotoxin, FB_1 is widely distributed in moldy grain and feed [20]. After the animal continues to ingest contaminated feed, FB_1 enters the body through the digestive tract. Thus, an intact digestive tract helps prevent toxins from entering the circulatory system and reduces the toxic effects of FB_1 [21]. IPEC-J2 cells are an in vitro model of the porcine intestine that can reflect the intestinal epithelial state when stimulated by FB_1 and provide insights into the effects of FB_1 on the porcine intestine.

The MTT results showed that when the FB_1 treatment time was extended to 48 h, cell survival rate decreased in a concentration-dependent manner. The cell viability of the 10 μg/mL treatment group increased, a result that may be due to the short-term stress on the cells. In our previous study, 50 μg/mL FB_1 also significantly reduced IPEC-J2 cell activity [19]. The morphology of cells can also reflect the degree of damage to cells. HE staining can enable us to observe the morphological changes in cells more clearly.

Cell cycle regulation is vital to cell proliferation, growth, and repair. The cell cycle is regulated by a variety of enzymes, proteins, cytokines, and cycle-related proteins [22]. CyclinD1 is an important protein in the G1 phase to S phase transition. It is expressed in early G1 phase and can bind to CDK4 or CDK6 to activate CDK2, enabling cells to pass the G1/S control point [23,24]. Anti-proliferative proteins such as P21 and P27 can inhibit the release of E2F by interacting with the cyclin/CDK complex [25]. Therefore, treatment of IPEC-J2 with FB_1 can reduce the expression of CDK2, CDK4, CyclinD1, and CyclinE1, preventing cells from passing through the G1/S control point and arresting the cell cycle in the G1 phase, thus inhibiting cell proliferation. In addition to IPEC-J2, FB_1 can inhibit the proliferation of a variety of cells. For example, pig spleen cells treated with FB_1 displayed IC_{50} at low concentrations, but FB_1 was less toxic to pig and human peripheral blood

mononuclear cells (PBMCs), and PBMC proliferation was inhibited by 50% only at higher concentrations of the toxin [26]. Our previous studies have shown that FB_1 inhibits SUVEC proliferation and prevents cells from entering the S phase from the G1 phase [15]. A variety of mycotoxins can affect cell proliferation, including AFB1 that can inhibit cell proliferation in porcine early embryonic development [27]. Similarly, 2000 mg/mL concentration of the Fusarium-derived mycotoxin deoxynivalenol (DON) significantly reduced the viability of IPEC-1 and IPEC-J2 cells and increased the proportion of cells in the G2/M phase [28].

Apoptosis is an evolutionarily conserved form of programmed cell death that is critical to animal development and tissue homeostasis [29]. Apoptosis includes type I apoptosis mediated by death receptors and type II apoptosis dependent on mitochondria [30]. In type II apoptosis, when mitochondria receive external stimuli, the membrane permeability of the mitochondria will change, and cytochrome C in mitochondria will be released into the cytoplasm to activate downstream apoptosis-related proteins. The expression of Caspase3 is one of the markers of apoptosis. Caspase3 is the upstream promoter of apoptosis. After cells receive apoptotic signals, Caspase3 activates the apoptotic executor Caspase9, thereby hydrolyzing a series of proteins and promoting apoptosis [31]. As a mycotoxin, FB_1 can produce toxic effects on a variety of cells and promote cell apoptosis. In our study, FB_1 significantly promoted the cleavage and expression of Caspase3 and Caspase9. Similarly, FB_1 induced apoptosis of HK-2 cells in a dose-dependent manner [32]. FB_1 at 50 μM (36 μg/mL) induced a large amount of DNA damage and chromatin depolymerization in SH-SY5y neuroblastoma cells, and also promoted nuclear translocation of apoptosis-inducing factors [33]. In terms of toxicity to animals, a significant increase in hepatocyte apoptosis was detected in mice fed with 5 mg/kg FB_1 for 42 days [34]. In conclusion, FB_1 displays cytotoxicity to a variety of animal cells and is capable of inducing apoptosis.

4. Conclusions

Our study demonstrated that FB_1 can cause injury to IPEC-J2 cells. The main manifestations of cell damage were cell number reduction, cell shrinkage, and floating. FB_1 can block the cell cycle and inhibit cell proliferation by reducing the expression of genes and proteins associated with the cell cycle (Figure 4). Meanwhile, FB_1 can induce apoptosis through the mitochondrial apoptosis pathway.
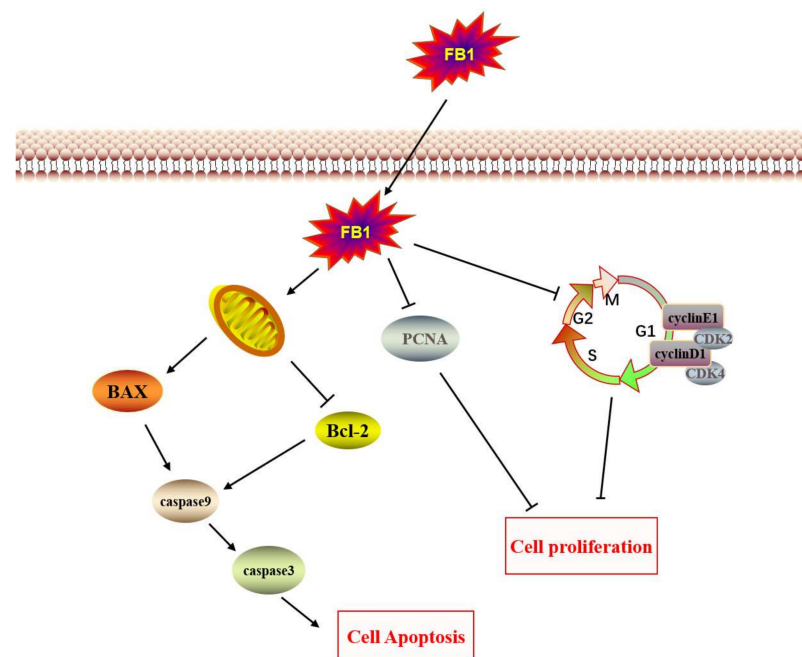

Figure 4. The supposed mechanism of toxic action of FB1 on IPEC-J2 cells.

5. Materials and Methods

5.1. Cells and Cell Culture

IPEC-J2 cells were bought from GuangZhou Jennio Biotech Co., Ltd. (Guangzhou, China). The cells were grown in DMEM (10% FBS + 1% penicillin/streptomycin). IPEC-J2 cells were cultured in an incubator at 37 °C with a continual supply of 5% CO_2.

5.2. Cell Viability Assay

Cell viability was determined using the 3-(4,5-dimethylthiazol-2yl)-2,5-diphenyltetrazolium bromide assay (MTT, CWBIO, Beijing, China). FB_1 (purity ≥ 98%, Sigma-Aldrich, St. Louis, MO, USA) was dissolved with dimethyl sulfoxide (DMSO, CWBIO) and its concentration was adjusted to 20 mg/mL. IPEC-J2 cells were seeded in cell culture plate and stimulated with different concentrations of FB_1 (0, 10, 20, and 40 µg/mL), and samples were incubated for 24 and 48 h. After the treatments, cells were washed with DMEM and then incubated in MTT solution (CWBIO, Beijing, China) for 2 h. The supernatant was removed after incubating for 2 h, and DMSO was added. Finally, the absorbance of the solution was measured at 490 nm in a spectrophotometer after 10 min.

5.3. Observation of Cell Morphology

An IPEC-J2 cell suspension was dropped into a 24-well plate and covered with a cell culture coverslip. Different concentrations of FB_1 (0, 10, 20, and 40 µg/mL) were added when the cell density reached 60%, and the IPEC-J2 cells were added with FB_1 and cultured for 48 h. The cell culture coverslip was taken for fixation, dehydration, transparency, hematoxylin, and eosin staining. The cells were observed under a light microscope.

5.4. Cell Proliferation Assay

For EdU labeling, an IPEC-J2 cell suspension was dropped into a 24-well plate. Different concentrations of FB1 (0, 10, 20, and 40 µg/mL) were added to the 24-well plate, and the cells were cultured for 48 h. IPEC cells were treated with 10 µM EdU for 2 h. For EdU staining, the cells were fixed with 4% paraformaldehyde, washed three times with PBS, and then incubated in 0.3% Triton® X-100(Beijing Solarbio Science and Technology Co., Ltd. Beijing, China) in PBS for 15 min at room temperature. The cells were then incubated with freshly-made Click-iT reaction cocktail for 15 min. Finally, images are taken under a fluorescence microscope.

5.5. RT-qPCR Analysis

Total RNA was isolated from IPEC-J2 cells by using TransZol Up reagent (TransGen Biotech, Beijing, China). Then, cDNA was synthesized using a reverse transcription kit according to manufacturer's instructions (TransGen Biotech). Real-time PCR was performed using Taq Pro Universal SYBR qPCR Master Mix (Vazyme Biotech Co., Ltd. Nanjing, China) and oligonucleotide primers (Table 1) on a Real-Time PCR Detection System (Applied Biosystems, Thermo Fisher Scientific, Waltham, MA, USA), and gene expression was calculated by the $2^{-\Delta\Delta Ct}$ method.

Table 1. Oligonucleotide primers used for real-time PCR.

Primer Name	Primer Sequences (5′-3′)	Primer Sequences
P21	F: 5′-3′ ACCCCTTCCCCATACCC R: 5′-3′TTCCTAACACCCATGAAACTG	XM_013977858.2
P27	F: 5′-3′GTCCCTTTCAGTGAGAACCG ATAC R: 5′-3′TTGCTGCCACATAACGGAATCAT	NM_214316.1
PCNA	F: 5′-3′GTGATTCCACCACCATGTTC R: 5′-3′TGAGACGACTCCATGCTCTG	NM_001291925.1

Table 1. *Cont.*

Primer Name	Primer Sequences (5′-3′)	Primer Sequences
cyclin D1	F: 5′-3′GCGAGGAACAGAAGTGCG R: 5′-3′TGGAGTTGTCGGTGTAGATGC	XM_021082686.1
cyclin E1	F: 5′-3′CTCGCCACTGCCTATACTGA R: 5′-3′GGTGCCGCTGCATAAGGT	XM_005653265.2
CDK2	F: 5′-3′GCGAGGAACAGAAGTGCG R: 5′-3′TGGAGTTGTCGGTGTAGATGC	XM_013977858.2
CDK4	F: 5′-3′GCGGAGATTGGTGTTGGTG R: 5′-3′CATTGGGGACTCTTACGCTCTT	NM_001123097.1
Caspase3	F: 5′-3′TGCTGCAAATCTCAGGGAGACCT R: 5′-3′GTGCCTCGGCAGGCCTGAAT	NM_214131.1
Caspase9	F: 5′-3′TGGCCTCGCTCTGGGATGCT R: 5′-3′TGGCCTCGCTCTGGGATGCT	NM_02107526.7
Bcl-2	F: 5′-3′CTGCGAACCCGGTCTGCCTG R: 5′-3′TCTCGGGCCCACTGCTCCTC	XM_005664627.3
Bax	F: 5′-3′CCGAGTGGCGGCCGAAATGT R: 5′-3′TCCAGCCCAGCAGCCGATCTG	XM_013998624.2
GAPDH	F: 5′-3′GTGATTCCACCACCATGTTC R: 5′-3′TGAGACGACTCCATGCTCTG	XM_021091114.1

5.6. Western Blot

Cells were treated with the above concentrations of FB_1 for 48 h, then washed three times with ice-cold PBS. The cells were then lysed with RIPA buffer (Solarbio) containing a protease inhibitor mixture (Solarbio, Beijing, China) and protein phosphatase inhibitor (Solarbio). The total protein concentrations were determined using a Bradford protein kit (Tiandz, Beijing, China). The total proteins were resolved by electrophoresis and transferred to poly(vinylidene fluoride) membranes for 80 min at 200 mA. PVDF membranes were incubated with primary antibodies caspase3 (Beijing Biosynthesis Biotechnology Co., Ltd. Beijing, China), caspase9 (Bioss), CDK2 (Bioss), CDK4 (Bioss, Beijing, China), cyclinD1(immunoway, Plano, TX 75024, USA), cyclinE1(immunoway), Bax (Proteintech Group, Inc., Wuhan, China), and GAPDH (Servicebio, Wuhan, China) overnight at 4 °C. Then, the membrane was washed three times with Tris-buffered saline tween (TBST) for 15 min. Secondary antibody (IgG, Vazyme) was used to incubate the membranes for 1 h at 4 °C. Finally, band density was quantified using the Image Lab 5.0 on the ChemiDOC XRS + system (Bio-Rad, Hercules, CA, USA).

5.7. Cell Cycle Assay

After 48 h of treatment with FB_1 (0, 10, 20, and 40 μg/mL), IPEC-J2 cells were suspended in ice-cold PBS after centrifugation. Then, 500 μL of propidium iodide (PI) solution (Genview, Beijing, China) was added to the sample and incubated for 30 min. Cells were analyzed using a flow cytometer.

5.8. Cell Apoptosis Assay

Apoptosis of IPEC-J2 cells was analyzed using a flow cytometer. Briefly, cells were treated with the above concentrations of FB_1 for 48 h, then washed three times with ice-cold PBS. The cells were stained with Annexin V/FITC-propidium iodide (PI), and the sample was incubated in the dark for 30 min. Cells were analyzed on a flow cytometer.

5.9. Δψm Determination

IPEC-J2 were treated with different concentrations of FB_1 for 48 h. Δψm of IPEC-J2 was observed by an inverted fluorescence microscope with a Δψm assay kit (Beyotime Biotech, Shanghai, China) according to the product's protocol.

5.10. Statistical Analysis

Results were expressed as mean $\pm$ standard deviation (SD). Comparisons between groups were made using *t*-test (two groups) and one-way analysis of variance (ANOV A). All experiments were repeated at least three times. A value of $p < 0.05$ was considered as a statistically significant difference (data marked with an asterisk *).

Author Contributions: H.L., J.S. and L.Z. designed the research; T.W., L.Z., M.T., Q.L. (Qing Liu), F.L. and Q.L. (Qing Li). performed the research, analyzed and interpreted the data; T.W. wrote the paper; J.S. and H.L. revised the paper. All authors have read and agreed to the published version of the manuscript.

Institutional Review Board Statement: Not applicable.

Informed Consent Statement: Not applicable.

Data Availability Statement: Not applicable.

Conflicts of Interest: The authors declare there is no conflict of interest.

References

1. Yang, C.; Song, G.; Lim, W. Effects of mycotoxin-contaminated feed on farm animals. *J. Hazard. Mater.* **2020**, *389*, 122087. [CrossRef] [PubMed]
2. Cao, C.; Zhu, X.; Li, X.; Ouyang, H.; Wang, K.; Li, X. Assessment of ionic homeostasis imbalance and cytochrome P450 system disturbance in mice during fumonisin B1 (FB1) exposure. *Chemosphere* **2020**, *251*, 126393. [CrossRef] [PubMed]
3. Mirón-Mérida, V.A.; González-Espinosa, Y.; Collado-González, M.; Gong, Y.Y.; Guo, Y.; Goycoolea, F.M. Aptamer–target–gold nanoparticle conjugates for the quantification of fumonisin B1. *Biosensors* **2021**, *11*, 18. [CrossRef] [PubMed]
4. Wang, X.; Wu, Q.; Wan, D.; Liu, Q.; Chen, D.; Liu, Z.; Martínez-Larrañaga, M.R.; Martínez, M.A.; Anadón, A.; Yuan, Z. Fumonisins: Oxidative stress-mediated toxicity and metabolism in vivo and in vitro. *Arch. Toxicol.* **2016**, *90*, 81–101. [CrossRef] [PubMed]
5. Bouhet, S.; Oswald, I.P. The intestine as a possible target for fumonisin toxicity. *Mol. Nutr. Food Res.* **2007**, *51*, 925–931. [CrossRef] [PubMed]
6. Prelusky, D.B.; Trenholm, H.L.; Rotter, B.A.; Miller, J.D.; Savard, M.E.; Yeung, J.M.; Scott, P.M. Biological fate of fumonisin B1 in food-producing animals. *Adv. Exp. Med. Biol.* **1996**, *392*, 265–278. [PubMed]
7. Bouhet, S.; Hourcade, E.; Loiseau, N.; Fikry, A.; Martinez, S.; Roselli, M.; Galtier, P.; Mengheri, E.; Oswald, I.P. The Mycotoxin fumonisin B1 alters the proliferation and the barrier function of porcine intestinal epithelial cells. *Toxicol. Sci.* **2003**, *77*, 165–171. [CrossRef]
8. Gao, S.; Liu, F. Novel insights into cell cycle regulation of cell fate determination. *J. Zhejiang Univ. Sci. B* **2019**, *20*, 467–475. [CrossRef]
9. Orford, K.W.; Scadden, D.T. Deconstructing stem cell self-renewal: Genetic insights into cell-cycle regulation. *Nat. Rev. Genet.* **2008**, *9*, 115–128. [CrossRef]
10. Strzalka, W.; Ziemienowicz, A. Proliferating cell nuclear antigen (PCNA): A key factor in DNA replication and cell cycle regulation. *Ann. Bot.* **2011**, *10*, 1127–1140. [CrossRef]
11. Gali-Muhtasib, H.; Bakkar, N. Modulating cell cycle: Current applications and prospects for future drug development. *Curr. Cancer Drug Targets* **2002**, *2*, 309–336. [CrossRef]
12. Wang, Z.; Wang, Y.; Wang, S.; Meng, X.; Song, F.; Huo, W.; Zhang, S.; Chang, J.; Li, J.; Zheng, B.; et al. Coxsackievirus A6 induces cell cycle arrest in G0/G1 phase for viral production. *Front. Cell. Infect. Microbiol.* **2018**, *8*, 279. [CrossRef]
13. Gao, X.; Leone, G.W.; Wang, H. Cyclin D-CDK4/6 functions in cancer. *Adv. Cancer Res.* **2020**, *148*, 147–169.
14. Li, Q.; Yuan, Q.; Wang, T.; Zhan, Y.; Yang, L.; Fan, Y.; Lei, H.; Su, J. Fumonisin B1 inhibits cell proliferation and decreases barrier function of swine umbilical vein endothelial cells. *Toxins* **2021**, *13*, 863. [CrossRef]
15. Gudipaty, S.A.; Conner, C.M.; Rosenblatt, J.; Montell, D.J. Unconventional ways to live and die: Cell death and survival in development, homeostasis, and disease. *Annu. Rev. Cell Dev. Biol.* **2018**, *34*, 311–332. [CrossRef]
16. Martin, S.J.; Green, D.R. Protease activation during apoptosis: Death by a thousand cuts? *Cell* **1995**, *82*, 349–352. [CrossRef]
17. Del Re, D.P.; Amgalan, D.; Linkermann, A.; Liu, Q.; Kitsis, R.N. Fundamental mechanisms of regulated cell death and implications for heart disease. *Physiol. Rev.* **2019**, *99*, 1765–1817. [CrossRef]
18. Chen, Z.; Zhou, L.; Yuan, Q.; Chen, H.; Lei, H.; Su, J. Effect of fumonisin B 1 on oxidative stress and gene expression alteration of nutrient transporters in porcine intestinal cells. *J. Biochem. Mol. Toxicol.* **2021**, *35*, e22706. [CrossRef]

19. Chen, Z.; Chen, H.; Li, X.; Yuan, Q.; Su, J.; Yang, L.; Ning, L.; Lei, H. Fumonisin B1 damages the barrier functions of porcine intestinal epithelial cells in vitro. *J. Biochem. Mol. Toxicol.* **2019**, *33*, e22397. [CrossRef]

20. Reisinger, N.; Schürer-Waldheim, S.; Mayer, E.; Debevere, S.; Antonissen, G.; Sulyok, M.; Nagl, V. Mycotoxin occurrence in maize silage—A neglected risk for bovine gut health? *Toxins* **2019**, *11*, 577. [CrossRef]

21. Akbari, P.; Braber, S.; Varasteh, S.; Alizadeh, A.; Garssen, J.; Fink-Gremmels, J. The intestinal barrier as an emerging target in the toxicological assessment of mycotoxins. *Arch. Toxicol.* **2017**, *91*, 1007–1029. [CrossRef]

22. Sun, Y.; Liu, Y.; Ma, X.; Hu, H. The influence of cell cycle regulation on chemotherapy. *Int. J. Mol. Sci.* **2021**, *22*, 6923. [CrossRef]

23. Clark, A.S.; Karasic, T.B.; DeMichele, A.; Vaughn, D.J.; O'Hara, M.; Perini, R.; Zhang, P.; Lal, P.; Feldman, M.; Gallagher, M.; et al. Palbociclib (PD0332991)—A selective and potent cyclin-dependent kinase inhibitor: A review of pharmacodynamics and clinical development. *JAMA Oncol.* **2016**, *2*, 253–260. [CrossRef]

24. Diehl, J.A. Cycling to cancer with cyclin D1. *Cancer Biol. Ther.* **2002**, *1*, 226–231. [CrossRef]

25. Xia, P.; Liu, Y.; Chen, J.; Cheng, Z. Cell cycle proteins as key regulators of postmitotic cell death. *Yale J. Biol. Mol.* **2019**, *92*, 641–650.

26. Taranu, I.; Marin, D.E.; Burlacu, R.; Pinton, P.; Damian, V.; Oswald, I.P. Comparative aspects of in vitro proliferation of human and porcine lymphocytes exposed to mycotoxins. *Arch. Anim. Nutr.* **2010**, *64*, 383–393. [CrossRef]

27. Shin, K.-T.; Guo, J.; Niu, Y.-J.; Cui, X.-S. The toxic effect of aflatoxin B1 on early porcine embryonic development. *Theriogenology* **2018**, *118*, 157–163. [CrossRef]

28. Diesing, A.K.; Nossol, C.; Panther, P.; Walk, N.; Post, A.; Kluess, J.; Kreutzmann, P.; Dänicke, S.; Rothkötter, H.J.; Kahlert, S. Mycotoxin deoxynivalenol (DON) mediates biphasic cellular response in intestinal porcine epithelial cell lines IPEC-1 and IPEC-J2. *Toxicol. Lett.* **2011**, *200*, 8–18. [CrossRef]

29. Cheng, X.; Ferrell, J.E. Apoptosis propagates through the cytoplasm as trigger waves. *Science* **2018**, *361*, 607–612. [CrossRef]

30. Schwabe, R.F.; Luedde, T. Apoptosis and necroptosis in the liver: A matter of life and death. *Nat. Rev. Gastroenterol. Hepatol.* **2018**, *15*, 738–752. [CrossRef]

31. Czabotar, P.E.; Lessene, G.; Strasser, A.; Adams, J.M. Control of apoptosis by the BCL-2 protein family: Implications for physiology and therapy. *Mol. Cell Biol.* **2014**, *15*, 49–63. [CrossRef] [PubMed]

32. Song, Y.; Liu, W.; Zhao, Y.; Zang, J.; Gao, H. Fumonisin B1 exposure induces apoptosis of human kidney tubular epithelial cells through regulating PTEN/PI3K/AKT signaling pathway via disrupting lipid raft formation. *Toxicon* **2021**, *204*, 31–36. [CrossRef] [PubMed]

33. Paul, S.; Jakhar, R.; Bhardwaj, M.; Chauhan, A.K.; Kang, S.C. Fumonisin B1 induces poly (ADP-ribose) (PAR) polymer-mediated cell death (parthanatos) in neuroblastoma. *Food Chem. Toxicol.* **2021**, *154*, 112026. [CrossRef] [PubMed]

34. Cao, C.; Xian, R.; Lin, F.; Li, X.; Li, X.; Qiang, F.; Li, X. Fumonisin B1 induces hepatotoxicity in mice through the activation of oxidative stress, apoptosis and fibrosis. *Chemosphere* **2022**, *296*, 133910. [CrossRef]